

The puzzling radio source in the cool core cluster A 2626

M. Gitti^{1,2,3*}

¹*Physics and Astronomy Department, University of Bologna, via Ranzani 1, 40127 Bologna, Italy*

²*INAF, Astronomical Observatory of Bologna, via Ranzani 1, 40127 Bologna, Italy*

³*INAF, Istituto di Radioastronomia di Bologna, via Gobetti 101, I-40129 Bologna, Italy*

Accepted 2013 August 14

ABSTRACT

We report on new VLA radio observations performed at 1.4 GHz and 4.8 GHz with unprecedented sensitivity and angular resolution (~ 1 arcsec) of the cool core cluster A 2626, which is known to possess a radio mini-halo at its center. The most unusual features of A 2626 are two elongated radio features detected in previous observations to the north and south, having morphologies not common to the typical jet-lobe structures in cool cores. In our new sensitive images the two elongated features appears clearly as bright radio arcs, and we discover the presence of a new arc to the west. These radio arcs are not detected at 4.8 GHz, implying a steep ($\alpha > 1$) spectrum, and their origin is puzzling. After subtracting the flux density contributed by these discrete features from the total flux measured at low resolution, we estimate a residual 18.0 ± 1.8 mJy flux density of diffuse radio emission at 1.4 GHz. We therefore confirm the detection of diffuse radio emission, which appears distinct from the discrete radio arcs embedded in it. Although its radio power is lower (1.4×10^{23} W Hz⁻¹) than previously known, the diffuse emission may still be classified as a radio mini-halo.

Key words: Galaxies: clusters: individual: Abell 2626 – Radio continuum: galaxies – galaxies: jets – galaxies: cooling flows

1 INTRODUCTION

The central dominant (cD) galaxies of cool core clusters have a high incidence of radio activity, showing the presence of central FR-I radiogalaxies in 70% of the cases (Burns 1990; Best et al. 2007; Mittal et al. 2009). Their behaviour differs from that of quasar: in many low-accretion-rate AGNs almost all the released energy is channelled into jets because the density of the gas surrounding the black hole is not high enough for an efficient radiation (e.g., Churazov et al. 2005). In fact, the importance of these objects has been underestimated for a long time due to their poor optical luminosity, and began to emerge after the discovery, with the X-ray satellite *ROSAT*, of deficits in the X-ray emission of the Perseus and Cygnus A clusters which are spatially coincident with regions of enhanced synchrotron emission (Boehringer et al. 1993; Carilli et al. 1994). With the advent of the new high-resolution X-ray observations performed with *Chandra* and *XMM-Newton*, it became clear that the central radio sources have a profound, persistent effect on the ICM – the central hot gas in many cool core systems is not smoothly distributed, but shows instead ‘holes’ on scales often approximately coincident with lobes of extended radio emission. The most typical configuration is for jets from the central dominant elliptical of a cluster to extend outwards in a bipolar flow, inflating lobes of radio-emitting plasma (radio ‘bubbles’). These lobes push aside the X-ray emitting gas of the cluster atmosphere, thus

excavating depressions in the ICM which are detectable as apparent ‘cavities’ in the X-ray images. Radio galaxies have thus been identified as a primary source of feedback in the hot atmospheres of galaxy clusters and groups (for recent reviews see Gitti et al. 2012; McNamara & Nulsen 2012, and references therein).

In some cases, the powerful radio galaxies at the center of cool core clusters are surrounded by diffuse radio emission on scales $\sim 200 - 500$ kpc having steep radio spectra ($\alpha > 1$; $S_\nu \propto \nu^{-\alpha}$). These radio sources, generally referred to as ‘radio mini-halos’, are synchrotron emission from GeV electrons diffusing through μ G magnetic fields. Although the central radio galaxy is the obvious candidate for the injection of the population of relativistic electrons, mini-halos do appear quite different from the extended lobes maintained by AGN, therefore their radio emission proves that magnetic fields permeate the ICM and at the same time may be indicative of the presence of diffuse relativistic electrons. In particular, due to the fact that the radiative lifetime of radio-emitting electrons ($\sim 10^8$ yr) is much shorter than any reasonable transport time over the cluster scale, the relativistic electrons responsible for the extended radio emission from mini-halos need be continuously re-energized by various mechanisms associated with turbulence in the ICM (re-accelerated *primary* electrons), or freshly injected on a cluster-wide scale (e.g. as a result of the decay of charged pions produced in hadronic collisions, *secondary* electrons). Gitti et al. (2002) developed a theoretical model which accounts for the origin of radio mini-halos as related to electron reacceleration by magnetohydrodynamic (MHD) turbulence, which is amplified by compression in

* E-mail: myriam.gitti@oabo.inaf.it

the cool cores. In this model, the necessary energetics to power radio mini-halos is supplied by the cooling flow process itself, through the compressional work done on the ICM and the frozen-in magnetic field. Although secondary electron models have been proposed to explain the presence of their persistent, diffuse radio emission on large-scale in the ICM (e.g., Pfrommer & Enßlin 2004; Keshet & Loeb 2010), the observed trend between the radio power of mini-halos and the maximum power of cooling flows (Gitti et al. 2004, 2012) has given support to a primary origin of the relativistic electrons radiating in radio mini-halos, favored also by the successful, detailed application of the Gitti et al. (2002) model to two cool core clusters (Perseus and A 2626, Gitti et al. 2004) and by recent statistical studies (Cassano et al. 2008). However, the origin of the turbulence necessary to trigger the electron reacceleration is still debated. The signatures of minor dynamical activity have recently been detected in some mini-halo clusters, thus suggesting that additional or alternative turbulent energy for the reacceleration may be provided by minor mergers (Gitti et al. 2007) and related gas sloshing mechanism in cool core clusters (Mazzotta & Giacintucci 2008; ZuHone et al. 2013).

Radio mini-halos are rare, with only about a dozen objects known so far (Feretti et al. 2012). The criteria initially adopted by Gitti et al. (2004) to select the first sample of mini-halo clusters, i.e. the presence of both a cool core and a diffuse, amorphous radio emission with no direct association with the central radio source, having size comparable to that of the cooling region, are now typically used to identify mini-halos. However, these criteria are somewhat arbitrary (in particular, total size, morphology, presence of cool core) and some identifications are still controversial. Furthermore, we stress that the classification of a radio source as a mini-halo is not trivial: their detection is complicated by the fact that the diffuse, low surface brightness emission needs to be disentangled from the strong radio emission of the central radio galaxy and of other discrete sources.

A 2626 is a low-redshift ($z=0.0553$, Struble & Rood 1999), regular, relatively poor Abell cluster (Mohr et al. 1996), with a double-nuclei cD elliptical galaxy (IC 5338) showing extended strong emission lines (Johnstone et al. 1987). Early observations with *Einstein* and *ROSAT*, then confirmed by *Chandra* and *XMM-Newton*, indicate that it hosts a moderate cooling flow (White et al. 1991; Rizza et al. 2000; Wong et al. 2008). Early, low resolution radio surveys showed that this cluster contains a central radio source exhibiting a compact unresolved core and a diffuse structure with very steep radio spectrum (Slee & Siegman 1983; Roland et al. 1985; Burns 1990). The compact radio component is associated with the southwest nucleus of the cD galaxy IC 5338 (Owen et al. 1995). More recently, high resolution VLA images of Gitti et al. (2004) highlighted the unusual properties of the A 2626 radio source. These authors found that at 1.4 GHz the central component consists of an unresolved core plus a small jet-like feature pointing to the south-western direction. The extended emission, that at lower resolution appears as a diffuse diamond-shaped emission detected up to $\sim 1'$ from the cluster center, is resolved out and two elongated parallel features of similar brightness and extent are visible. The total flux density of these ‘bar’ structures is ~ 6.6 mJy, contributing to $\sim 20\%$ of the flux of the diffuse radio emission detected at low resolution. Such symmetric, elongated features are imaged also by low resolution observations at 330 MHz, with a total flux density (including the diffuse emission) of ~ 1 Jy, whereas no radio emission is detected at the location of the core. Gitti et al. (2004) argue that the two unusual elongated features are distinct from and embedded in the diffuse extended radio emission, which they clas-

Table 1. New VLA data analyzed in this paper (project code: AG795, PI: M. Gitti)

Obs. Date	Band	Frequency (MHz)	Bandwidth (MHz)	Array	TOS (h)
08-Nov-21	C	4885.1/4835.1	50.0	A	3.5
09-Apr-30	C	4885.1/4835.1	50.0	B	3.5
08-Nov-22	L	1464.9/1385.1	50.0	A	5.0
09-May-04	L	1464.9/1385.1	50.0	B	7.0

sified as a radio mini-halo and successfully modeled as radio emission from relativistic electrons reaccelerated by MHD turbulence in the cooling core region. On the other hand, the origin and nature of the two radio bars is not clear as they are not associated to any X-ray cavities (Wong et al. 2008).

In this paper we present new high-resolution VLA data of the central radio source in A 2626, whose morphology much complex than that of the standard X-ray radio bubbles seen in other cool core clusters represents a challenge to models for the ICM - radio source interaction. With $H_0 = 70$ km s $^{-1}$ Mpc $^{-1}$, and $\Omega_M = 1 - \Omega_\Lambda = 0.3$, the luminosity distance of A 2626 is 246.8 Mpc and 1 arcsec corresponds to 1.1 kpc.

2 OBSERVATIONS AND DATA REDUCTION

We performed new Very Large Array¹ observations of the radio source A 2626 at 1.4 GHz and 4.8 GHz in A- and B-configuration (see Table 1 for details regarding these observations). In all observations the source 3C 48 (0137+331) was used as the primary flux density calibrator, while the sources 0016–002 and 3C 138 (0521+166) were used as secondary phase and polarization calibrators, respectively. Data reduction was done using the NRAO AIPS (Astronomical Image Processing System) package, version 31DEC13. Accurate editing of the (u,v) data was applied with the task TVFLG to identify and remove bad visibility points. Images were produced by following the standard procedures: Calibration, Fourier-Transform, Clean and Restore. Self-calibration with the task CALIB was applied to remove residual phase variations.

The four datasets, taken at different frequencies and with different configurations, were reduced separately in order to optimize the accuracy of data editing and (self-)calibration of each single observation. In order to fully exploit the relative advantages in terms of angular resolution and sensitivity of the two VLA configurations used for the observations, we then combined together (with the task DBCON) the resulting (u,v) data in A- and B- configuration taken at the same frequency. On these combined A+B datasets, one at 1.4 GHz and one at 4.8 GHz, we also performed a few more iterations of self-calibration to improve the dynamic range of the images. We produced images in the Stokes parameters I, Q and U at different resolutions by specifying appropriate values of the parameters UVTAPER and ROBUST in the AIPS task IMAGR. The images of the polarized intensity, the fractional polarization and the position angle of polarization were derived from the I, Q and U images. The final maps show the contours of the total intensity.

¹ The Very Large Array (VLA) is a facility of the National Radio Astronomy Observatory (NRAO). The NRAO is a facility of the National Science Foundation, operated under cooperative agreement by Associated Universities, Inc.

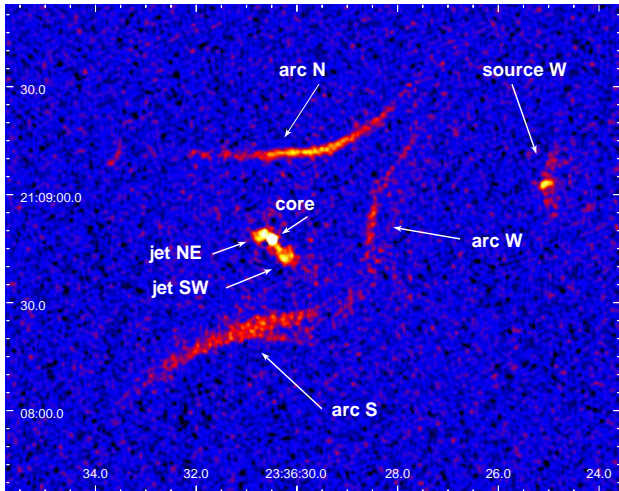


Figure 1. 1.4 GHz VLA map of A2626 at a resolution of $1''.2 \times 1''.2$, obtained by setting the parameter `ROBUST=-5`, `UVTAPER=0`. The r.m.s. noise is 0.012 mJy/beam and the peak flux density is 12.9 mJy/beam. The arrows indicate the features discussed in the text.

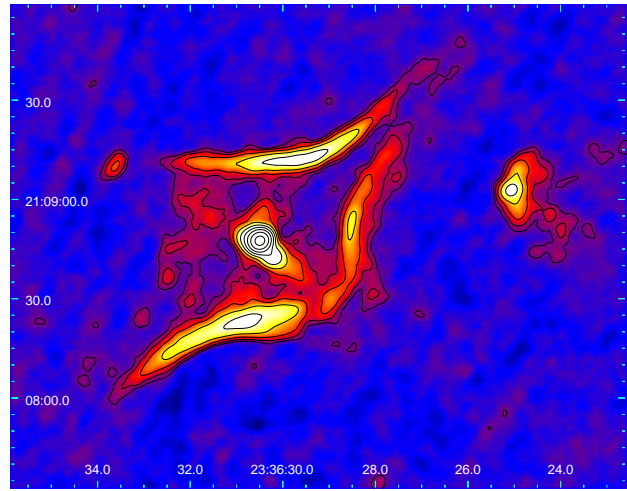


Figure 3. 1.4 GHz VLA map of A2626 at a resolution of $4''.4 \times 3''.9$ (the beam is shown in the lower-left corner), obtained by setting the parameter `ROBUST=5`, `UVTAPER=90`. The r.m.s. noise is 0.014 mJy/beam and the peak flux density is 14.0 mJy/beam. The contour levels are the same as in Fig. 2.

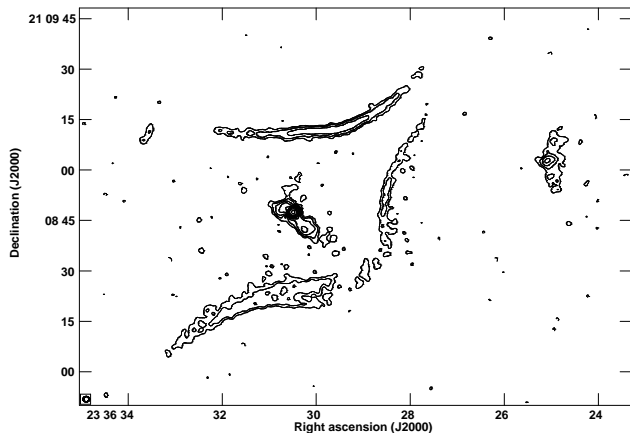


Figure 2. *Left:* 1.4 GHz VLA map of A2626 at a resolution of $1''.7 \times 1''.6$ (the beam is shown in the lower-left corner), obtained by setting the parameter `ROBUST=0`, `UVTAPER=0`. The r.m.s. noise is 0.010 mJy/beam and the peak flux density is 13.1 mJy/beam. The contour levels are -0.04 (dashed), 0.04, 0.08, 0.16, 0.32, 0.64, 1.28, 2.56, 5.12, 10.24 mJy/beam.

For the only purpose of deriving the total flux density of the radio source, including the diffuse emission, we also analyzed old 1.4 GHz data obtained with the VLA in C-configuration (Proj. code AM735, PI: T. Markovic). In this 3.5 h archival observation, performed in spectral-line mode, the source 3C 48 was used as the primary flux density calibrator, while the source 0204+152 was used as secondary phase calibrator.

Typical amplitude calibration errors are at 3%, therefore we assume this uncertainty on the flux density measurements.

3 RESULTS

Figure 1 shows the 1.4 GHz radio image of A2626 at full resolution (restoring beam of $1''.2 \times 1''.2$), obtained with pure uniform weighting by setting `ROBUST=-5`, whereas Figure 2 shows the contour map obtained by tempering the uniform weights with `ROBUST=0` (restoring beam of $1''.7 \times 1''.6$), which slightly improved the dy-

namic range of the image. With these high resolutions it is possible to image the central source and to spot the presence of other discrete features that can contribute to the total flux density and extended morphology detected at lower resolution. The nuclear source, located at RA (J2000): $23^{\text{h}} 36^{\text{m}} 30^{\text{s}}.5$, Dec (J2000): $21^{\circ} 08' 47''.6$, is here fully unveiled: it clearly shows two jets pointing to the northeast-southwest direction, extending out from the unresolved core to a distance of approximately 5 kpc. The total flux density of the core-jets structure is 17.7 ± 0.5 mJy. In these sensitive images the already known elongated radio features stand out very clearly as bright radio arcs (arc N and arc S in Fig. 1). They are symmetrically located at ~ 25 kpc to the north and south of the core, showing total longitudinal extensions of approximately 70 and 62 kpc, respectively. Their combined total flux density is 16.2 ± 0.5 mJy, which is a factor ~ 2.5 higher than previously estimated (Gitti et al. 2004). Furthermore, we identify a new feature which was not detected in the previous observations: a faint (3.1 ± 0.1 mJy), elongated arc to the west of the core (arc W in Fig. 1), which extending for about 60 kpc appears to ideally connect the western edges of the two radio arcs N-S. No diffuse emission is seen at this high resolution and no significant polarized flux is detected at 1.4 GHz at any resolution.

We produced an image at the lower resolution of $4''.4 \times 3''.9$, obtained with tapered natural weighting by setting `ROBUST=5` and `UVTAPER=90` (Fig. 3), to better map the extended structures. Diffuse 1.4 GHz emission appears clearly surrounding the nucleus in the region encompassed by the features (arc N, arc S and arc W) discussed above. In order to estimate correctly the flux density of the diffuse emission, we analyzed the archival C-array data and produced a 1.4 GHz map at a resolution of $14''.4 \times 12''.6$ (not shown here). The total source A 2626 imaged with this low resolution has a well-known diamond-like shape extending for approximately $2'.9 \times 2'.0$ (156×135 kpc), with a total flux density of 55.0 ± 1.7 mJy (source W excluded), in agreement with previous observations (Ledlow & Owen 1995; Rizza et al. 2000). By subtracting the emission contributed by the discrete features seen at high resolution (core + jets + arcs = 37.0 ± 0.6 mJy, see Table 2) from the total flux density of the C-array 1.4 GHz emission, we

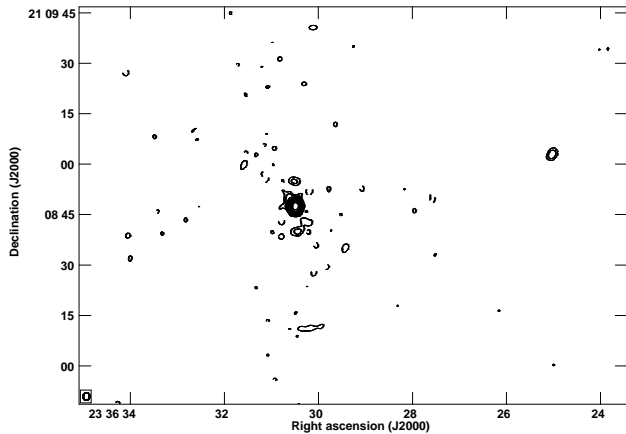


Figure 4. 4.8 GHz VLA map of A2626 at a resolution of $2''.3 \times 2''.0$ (the beam is shown in the lower-left corner), obtained by setting the parameter ROBUST=5, UVTAPER=90. The r.m.s. noise is 0.012 mJy/beam and the peak flux density is 9.5 mJy/beam. The contour levels are the same as in Fig. 2 and the map size in the same as Figs. 1-3.

thus measure a residual flux density of diffuse radio emission of 18.0 ± 1.8 mJy.

The more crude approach of measuring directly the flux density inside the contours of the diffuse emission visible in the map in Fig. 3 would provide an estimate of ~ 5 mJy. However, we note that this is certainly a lower limit as the A+B array data misses the flux contribution of the short baselines which are instead present in the C- array data, thus losing sensitivity to diffuse radio structures. We also attempted to derive the flux of the discrete features from the C- array map directly, getting a rough estimate of ~ 40 mJy (unresolved central component + arcs). Considering the difficulty in separating the emission from each component at low resolution, leading to big uncertainties, this estimate should be considered not far from the accurate one derived from our high resolution A+B array data. The variety of methods discussed here demonstrates the complexity of disentangling the relative contribution of the diffuse emission and of the discrete sources to the total observed radio emission.

Figure 4 shows the 4.8 GHz radio image of A 2626 at a resolution of $2''.3 \times 2''.0$, obtained with tapered natural weighting by setting ROBUST=5 and UVTAPER=90. At this higher frequency only the central component is visible, showing an unresolved core plus jet-like features pointing to the northeast-southwest directions². The total flux density is 9.8 ± 0.3 mJy (jet-like features included). The core appears slightly polarized at a level of $\sim 4\%$. The three discrete arcs seen at 1.4 GHz are not detected, implying a steep spectral index (see Table 2).

We finally note that a discrete source is visible to the west of A 2626 in all radio maps (source W in Fig. 1), located at RA(J2000): $23^{\text{h}}36^{\text{m}}25^{\text{s}}.1$, Dec(J2000): $21^{\circ}09'03''$, which is associated to the cluster S0 galaxy IC 5337. The morphology of this source suggests that it is a head-tail radio galaxy.

The radio results are summarized in Table 2, where we also report the 1.4 GHz monochromatic radio power.

Table 2. Summary of radio results for A 2626. The sizes are estimated from the maps at 1.4 GHz, and the flux densities are estimated inside the 3σ contour level (for the core measurements, we performed a gaussian fit with the task JMFIT). The superscripts ⁽¹⁾, ⁽²⁾ and ⁽⁴⁾ indicate that the flux is measured from Fig. 1, Fig. 2 and Fig. 4, respectively. When no emission is detected at 4.8 GHz, the spectral index is estimated assuming an upper limit of 3σ . The 1.4 GHz monochromatic radio power is in unit of 10^{23} W Hz^{-1} and the associated error is at 3%.

Source	Size ($''^2$)	$S_{1.4}$ (mJy)	$S_{4.8}$ (mJy)	$\alpha_{1.4}^{4.8}$ ($S_{\nu} \propto \nu^{-\alpha}$)	$P_{1.4}$
Core	unresolved	13.5 ± 0.4 ⁽¹⁾	9.6 ± 0.3 ⁽⁴⁾	0.28 ± 0.03	1.06
Jet NE	$\sim 5 \times 5$	1.9 ± 0.1 ⁽¹⁾	~ 0.1 ⁽⁴⁾	~ 2.4	0.15
Jet SW	$\sim 6 \times 4$	2.3 ± 0.1 ⁽¹⁾	~ 0.1 ⁽⁴⁾	~ 2.6	0.18
Arc N	$\sim 64 \times 4$	7.2 ± 0.2 ⁽²⁾	– ⁽⁴⁾	> 1.6	0.57
Arc S	$\sim 56 \times 6$	9.0 ± 0.3 ⁽²⁾	– ⁽⁴⁾	> 1.0	0.71
Arc W	$\sim 55 \times 3$	3.1 ± 0.1 ⁽²⁾	– ⁽⁴⁾	> 1.0	0.24

4 DISCUSSION AND CONCLUSIONS

4.1 Radio Arcs

Since their discovery (Gitti et al. 2004), the nature of the two elongated radio features to the north and south directions (arc N and arc S in Fig. 1) has been a puzzle. Their symmetric positions on each side of the core suggests that they are radio bubbles, but their thin, elongated shapes are unlike those typically observed in cool core clusters. They may represent radio emitting plasma injected by the central source during an earlier active phase, which has then propagated through the cool core region in the form of buoyant subsonic plumes (e.g., Gull & Northover 1973; Churazov et al. 2000; Brüggén & Kaiser 2001). However, such plumes are expected to have a torus-like concavity (Churazov et al. 2000), contrarily to the observed shape in A 2626. Furthermore, by comparison to radio lobes and bubbles associated with other cool core dominant radio galaxies, one might expect these to be regions of reduced X-ray emission surrounded by bright rims. In fact, previous *ROSAT* observations failed to find strong X-ray deficit in the cool core of A 2626 (Rizza et al. 2000). Recently, this cluster has been studied in more detail with *Chandra* and *XMM-Newton*, but yet no X-ray cavities associated with the elongated radio features have been found (Wong et al. 2008).

Wong et al. (2008) argue that the lack of obvious correlation between the two symmetric parallel radio features and any structures in the X-ray images may indicate that they are thin tubes parallel to the plane of the sky, or that the radio plasma is mixed with the X-ray gas, rather than displacing it. These authors suggest that jet precession might also provide an alternative explanation of the peculiar radio morphology. If two jets ejected towards the north and south by the southwest cD nucleus are precessing about an axis which is nearly perpendicular to the line-of-sight and are stopped at approximately equal radii from the AGN (at a ‘working surface’), radio emission may be produced by particle acceleration, thus originating the elongated structures. The impressive arc-like, symmetric morphology of these features highlighted by the new high resolution radio images may support this interpretation.

The discovery of a third elongated feature to the west (arc W in Fig. 1) further complicates the picture. It could represent another radio bubble ejected in a different direction, similarly to what observed in RBS 797 (Gitti et al. 2006), but again the absence of any correlation with the X-ray image and its “wrong” concavity, as well as the absence of its counterpart to the east, disfavor this interpretation. In the model proposed by Wong et al. (2008), it could also represent the result of particle acceleration produced at a working

² Given the pattern of the dirty beam, the two ‘blobs’ visible to the north and south of the core are likely to be image artifacts

surface by a third jet ejected to the west. This interpretation would imply the existence of radio jets emanating also from the northeast nucleus (separated by only ~ 4 kpc from the active southwest nucleus) of the cD galaxy IC 5338, which however does not show a radio core.

We stress that the radio arcs have an elongated morphology and steep spectral index (see Table 2). These characteristics are similar to those of cluster radio relics associated to particle reacceleration due to shocks (Feretti et al. 2012). We also note that each arc resembles the morphology of the large-scale structure of the radio source 3C 338, which is disconnected from the core emission having two-sided jets and has been interpreted as a relic structure not related to the present nuclear activity (Giovannini et al. 1998). The presence of three such arcs in A 2626 makes the interpretation even more puzzling. Seen all together, the combined shape of the three arcs suggests that they could trace the symmetric fronts of a single elliptical shock originating from the core. However, we notice again that their concavity is not what one would expect from a shock propagating from the center. If they are cluster radio relic-like sources due to reacceleration at a bow shock, the observed concavity suggests that three distinct shocks should be propagating toward the center from different directions. However, the presence of such symmetric shocks in the atmosphere of a relatively relaxed cluster seems very unlikely, given also that *Chandra* observations failed to detect any obvious X-ray edge ascribable to shock fronts. Furthermore, relic sources are typically strongly polarized (Feretti et al. 2012), whereas no significant polarized flux is detected in our data (see Sect. 3).

It is also possible that the nature of the two bright radio arcs N-S is different from that of the fainter arc W, which lacks an obvious counterpart to the east and could be related to the merging of the nearby S0 galaxy IC 5337 (see Fig. 16 of Wong et al. (2008) for a possible correlation with the *Chandra* hardness ratio map). Therefore the complex morphology of the A 2626 radio source may result from a combination of the scenarios presented above.

As it appears evident from this discussion, the new high-resolution VLA data are not definitive to solve the puzzle of the origin and nature of the radio arcs in A 2626.

4.2 Diffuse radio emission

With the new sensitive observations presented here, which improve by a factor ~ 3 the r.m.s. noise of the published maps (Gitti et al. 2004), we confirm the detection of diffuse 1.4 GHz emission, having a radio power of $P_{1.4} = 1.4 \times 10^{23}$ W Hz $^{-1}$. As imaged at this high resolution ($\sim 4''$), the diffuse radio emission appears to be confined in the region encompassed by the three radio arcs, surrounding the nucleus, and shows a fragmented morphology with total size ~ 60 kpc.

Although lower than previously estimated, the radio power of the diffuse emission in A 2626 still follows the trend with the maximum power of cooling flows, which is expected in the framework of the model proposed by Gitti et al. (2002, 2004). This model links the origin of radio mini-halos to radio emission from relativistic electrons reaccelerated by Fermi mechanism associated with MHD turbulence amplified by the compression of the magnetic field in the cooling core region, thus supporting a direct connection between cool cores and radio mini-halos (see Fig. 3b of Gitti et al. (2012) for a recent version of the observed trend).

The relativistic electrons responsible for the diffuse emission may also have been reaccelerated by turbulence generated by the sloshing of the cool core gas (Mazzotta & Giacintucci 2008; ZuHone et al. 2013). The presence of three symmetric sloshing

sub-clumps in the cluster atmosphere, although unlikely, might also induce local electron (re)acceleration thus explaining the origin of the three radio arcs discussed in Sect. 4.1.

ACKNOWLEDGMENTS

MG thanks G. Giovannini and D. Dallacasa for helpful advices during the data reduction, and S. Giacintucci and K. Wong for providing comments on the original manuscript. MG acknowledges the financial contribution from contract ASI-I/009/10/0.

REFERENCES

- Best P. N., von der Linden A., Kauffmann G., Heckman T. M., Kaiser C. R., 2007, *MNRAS*, 379, 894
- Boehringer H., Voges W., Fabian A. C., Edge A. C., Neumann D. M., 1993, *MNRAS*, 264, L25
- Brüggen M., Kaiser C. R., 2001, *MNRAS*, 325, 676
- Burns J. O., 1990, *AJ*, 99, 14
- Carilli C. L., Perley R. A., Harris D. E., 1994, *MNRAS*, 270, 173
- Cassano R., Gitti M., Brunetti G., 2008, *A&A*, 486, L31
- Churazov E., Forman W., Jones C., Böhringer H., 2000, *A&A*, 356, 788
- Churazov E., Sazonov S., Sunyaev R., Forman W., Jones C., Böhringer H., 2005, *MNRAS*, 363, L91
- Feretti L., Giovannini G., Govoni F., Murgia M., 2012, *A&A Rev.*, 20, 54
- Giovannini G., Cotton W. D., Feretti L., Lara L., Venturi T., 1998, *ApJ*, 493, 632
- Gitti M., Brighenti F., McNamara B. R., 2012, *Advances in Astronomy*, 2012
- Gitti M., Brunetti G., Feretti L., Setti G., 2004, *A&A*, 417, 1
- Gitti M., Brunetti G., Setti G., 2002, *A&A*, 386, 456
- Gitti M., Feretti L., Schindler S., 2006, *A&A*, 448, 853
- Gitti M., Ferrari C., Domainko W., Feretti L., Schindler S., 2007, *A&A*, 470, L25
- Gull S. F., Northover K. J. E., 1973, *Nature*, 244, 80
- Johnstone R. M., Fabian A. C., Nulsen P. E. J., 1987, *MNRAS*, 224, 75
- Keshet U., Loeb A., 2010, *ApJ*, 722, 737
- Ledlow M. J., Owen F. N., 1995, *AJ*, 109, 853
- Mazzotta P., Giacintucci S., 2008, *ApJ*, 675, L9
- McNamara B. R., Nulsen P. E. J., 2012, *New Journal of Physics*, 14, 055023
- Mittal R., Hudson D. S., Reiprich T. H., Clarke T., 2009, *A&A*, 501, 835
- Mohr J. J., Geller M. J., Wegner G., 1996, *AJ*, 112, 1816
- Owen F. N., Ledlow M. J., Keel W. C., 1995, *AJ*, 109, 14
- Pfommer C., Enßlin T. A., 2004, *A&A*, 413, 17
- Rizza E., Loken C., Bliton M., Roettiger K., Burns J. O., Owen F. N., 2000, *AJ*, 119, 21
- Roland J., Hanisch R. J., Veron P., Fomalont E., 1985, *A&A*, 148, 323
- Slee O. B., Siegman B. C., 1983, *Proceedings of the Astronomical Society of Australia*, 5, 114
- Struble M. F., Rood H. J., 1999, *ApJS*, 125, 35
- White D. A., Fabian A. C., Johnstone R. M., Mushotzky R. F., Arnaud K. A., 1991, *MNRAS*, 252, 72
- Wong K.-W., Sarazin C. L., Blanton E. L., Reiprich T. H., 2008, *ApJ*, 682, 155
- ZuHone J. A., Markevitch M., Brunetti G., Giacintucci S., 2013, *ApJ*, 762, 78